Food Hydrocolloids 145 (2023) 109059

Contents lists available at ScienceDirect

Food Hydrocolloids

journal homepage: www.elsevier.com/locate/foodhyd

Formation and properties of highly concentrated oil-in-water emulsions stabilised by emulsion droplets

Lirong Cheng [a], Aiqian Ye [a,*], Zhi Yang [b], Yacine Hemar [c], Harjinder Singh [a]

[a] Riddet Institute, Massey University, Private Bag 11 222, Palmerston North, 4442, New Zealand
[b] School of Food and Advanced Technology, Massey University, Auckland, 0632, New Zealand
[c] Institute for Advanced Study, Shenzhen University, Shenzhen, 518060, China

ARTICLE INFO

Keywords:
Droplet-stabilised emulsion
Interfacial structure
Calcium caseinate particles
Emulsion gels
Rheology

ABSTRACT

70% (v/v) concentrated emulsion has been prepared using Ca^{2+}-cross-linked sodium caseinate particles (Ca-CAS) or Ca-CAS coated nano-sized primary emulsion droplets as emulsifiers. The primary droplet-stabilised emulsion (DSE) was compared with the conventional Ca-CAS stabilised-emulsion (PSE) in terms of viscoelasticity as affected by aging (30 days) and heating (80 °C, 30 min) at pH 5.8 and 7.0. DSE at pH 5.8 showed the highest complex modulus ($G^* = 1174 \pm 39$ Pa), approximately was six-times higher than other emulsions ($G^* \leq \sim 250$ Pa) due to the thick emulsifier layer consisting of primary droplet increasing the effective volume faction of core droplets by a factor of ~1.21. After aging, G^* of DSE at pH 5.8 increased to 1685 ± 68 Pa, while G^* of other three emulsions were ~400 Pa. After heating, G^* of DSE reached 1801 ± 69 Pa and 1312 ± 205 Pa at pH 5.8 and pH 7.0, respectively, while G^* of PSE were ~600 Pa at both pHs. The possible mechanism for aging-induced gelation was the gravity-driven microphase separation, in which the droplets flocculate together with the entrapped aqueous phase increasing the effective volume fraction. The heat-induced gelation was attributed to the increase in droplet interactions through protein aggregates and/or primary droplets forming three-dimensional networks at elevated temperature. This study suggests that the mechanical strength of food-grade concentrated emulsions can be effectively improved using nano-sized primary emulsions as emulsifying agent and can be further modulated by aging or heating, which will be useful for developing semi-solid emulsion-based products.

1. Introduction

Oil-in-water (O/W) emulsion is a mixture of two immiscible liquid phases, with one oil phase dispersed as droplets in another aqueous continuous phase. When the volume fraction of the disperse phase (φ) is high, the droplets are packed very closely, conferring the emulsion a yield-stress and viscoelastic properties. Typically, they appear to flow at high shear rates but solidify at low shear rates, exhibiting high stability with a self-supporting texture (Li et al., 2020). Owing to the unique gel-like rheological properties, special texture and long-term stability, concentrated emulsions have attracted increasing attention from both academic research and industry (Li et al., 2018; Patel & Dewettinck, 2016). The advantages of concentrated emulsion rely on their adjustable viscoelastic properties (Tan et al., 2020; Wang et al., 2016). Many studies have indicated that the rheological properties of concentrated emulsion depend on φ (Hemar & Horne, 2000; Lacasse et al., 1996; Mason et al., 1996; Princen & Kiss, 1986), droplet size distribution (Desmond & Weeks, 2014; Foudazi et al., 2012; Pal, 1996), droplet coalescence and aggregation state (Berli, 2007; Chuang et al., 2020; Zhang et al., 2021), as well as continuous phase viscosity (Geremias-Andrade et al., 2017; Zhu et al., 2019). These factors can be manipulated prior to emulsification by adjusting different parameters such as emulsifiers, oil fraction, pH, ionic strength, additives, etc., to obtain a concentrated emulsion with desirable processibility, physicochemical and functional properties. For instance, a reduced disperse phase volume fraction of emulsion could be designed to have the same rheological properties than that made with a higher disperse phase volume fraction.

The viscoelasticity of concentrated emulsions could change over long-term storage, due to droplets coalescence (Chuang et al., 2020; Dimitrova & Leal-Calderon, 2004; Hu et al., 2016). To improve the long-term stability towards coalescence of concentrated emulsions, strategies using large amount of surfactants (e.g., Tweens and Spans) (Barbetta & Cameron, 2004; Cameron & Sherrington, 1996; Wijaya et al., 2017) or colloidal particles (e.g., silica particles) (Abdullah et al.,

* Corresponding author. Riddet Institute, Massey University, Private Bag 11 222, Palmerston North 442, New Zealand.
E-mail address: A.M.Ye@massey.ac.nz (A. Ye).

https://doi.org/10.1016/j.foodhyd.2023.109059
Received 12 April 2023; Received in revised form 17 June 2023; Accepted 6 July 2023
Available online 13 July 2023

Abbreviations

Ca-CAS	Ca^{2+}-cross-linked sodium caseinate
CLSM	confocal laser scanning microscopy
DSE	droplet-stabilised emulsion
DLS	dynamic light scattering
PDI	polydisperse index
PSE	protein-stabilised emulsion
φ	volume fraction of the disperse phase
SDS	sodium dodecyl sulphate
SLS	static light scattering

2020; Zheng et al., 2014) are often employed. It is well established that emulsions stabilised by colloidal particles often possess better stability to droplet coalescence than those stabilised by surfactants through Pickering mechanism (Binks, 2002). Therefore, the application of food-grade particles (e.g., starch, cellulose, chitin, proteins, and polysaccharides) has attracted increased interest in the manufacture of edible concentrated emulsion-based products (Huang et al., 2019; Zhang et al., 2021; Zhu et al., 2019). However, a low viscoelasticity of about 10–500 Pa at 1 Hz has been usually reported for Pickering concentrated emulsions ($\varphi > 0.75$) that are stabilised by food-grade particles, such as gliadin-based particles (Zeng et al., 2017), zein-based particles (Jiang et al., 2019), whey protein microgel (Su et al., 2018), and pH-modified casein particles (Guo et al., 2021).

Recently, several studies have been carried out to improve the mechanical strength of concentrated emulsions through modifying the interfacial structure by increasing the size of the particles and improving the amount of the adsorbed particles at the interface (Guo et al., 2021; Yan et al., 2019). For example, concentrated emulsions stabilised with OSA starch/chitosan complex particles showed the highest viscoelasticity at pH 6 as compared to emulsions formed at pH below 6. At pH 6, the OSA starch/chitosan particle had a large size and formed a thick interfacial layer at the droplet surfaces, which promote the formation of a percolation network structure in the emulsion (Yan et al., 2019). Similar results have been found in zein/pectin hybrid particle (ZPHP)-stabilised Pickering emulsions (Zhou et al., 2018). A well-ordered interfacial layer of the droplet formed with ZPHP at pH 3.0 led to high interfacial coverage and a better stability and higher viscoelasticity compared to emulsions formed at higher pH. It has been suggested that the protective well-ordered and thick interfacial layer contribute to the formation of a percolating network of droplets and thus to the viscoelastic properties of concentrated emulsions (Yan et al., 2019; Zhou et al., 2018). This type of interfacial layer has been previously observed in dilute emulsion ($\varphi = 0.2$) formed with small primary droplets as emulsifying agent (Cheng et al., 2019; Ye et al., 2013). Emulsion droplets has also been used to strength the adsorbed protein layer at the air bubble surface and enhanced stability of air bubble against to coalescence (Murray et al., 2009). This leads one to hypothesise that the viscoelasticity of the concentrated emulsion will be improved by the formation of a thick interfacial layer consisting of small primary droplets.

The aim of this study was therefore to develop an oil-in-water concentrated emulsion (70% v/v) stabilised by primary droplets coated with calcium cross-linked caseinate particles (Ca-CAS) with different interfacial structures. The concentrated emulsions stabilised by Ca-CAS coated primary droplets were compared to emulsions solely stabilised by Ca-CAS in terms of their rheological properties at controlled compositions (e.g., same oil volume fraction and protein concentration). The effects of aging (30 days) and heating (80 °C, 30 min) on the rheological properties were also investigated. The rheological measurements were supported with droplet size measurements and confocal laser scanning microscopy observation.

2. Materials and methods

2.1. Materials

Sodium caseinate (Alanate 180: 92.7% w/w protein, 4.3% w/w moisture, 0.7% w/w fat and 0.2% w/w carbohydrate) was purchased from Fonterra Co-operative Group Ltd. (Auckland, New Zealand). Soybean oil was purchased from Davis Trading Company, Palmerston North, New Zealand. Milli-Q water (Millipore Corp., Bedford, MA, USA) was used for all experiments. All chemicals used were of analytical grade and were purchased from Sigma-Aldrich (St. Louis, MO, USA) or BDH Chemicals (BDH Ltd., Pooles, England) unless otherwise specified.

2.2. Preparation of calcium cross-linked caseinate particles

Stock sodium caseinate (CAS) dispersion with protein concentration of 3.1 w/v% was prepared by dissolving sodium caseinate powder in ultrapure Milli-Q water (18.2 MΩ) at 50 °C and stirring for 2 h, followed by overnight storage at the room temperature to ensure complete hydration. The pH of this sodium caseinate dispersion was 6.90 ± 0.2. The Ca-CAS dispersion was prepared by adding an appropriate amount of stock $CaCl_2$ solution (1 M, 0.22 μm filtration) dropwise to the stock CAS dispersion under mild stirring, equilibrating at room temperature for half-hour, and then adjusting the pH to 7.00 ± 0.05 using 2 M NaOH or 2 M HCl and equilibrating at room temperature overnight. The final Ca-CAS dispersion contains 3.0% w/v protein and 20 mM $CaCl_2$, which is close to the concentration of protein and colloidal calcium found in casein micelles (Williams et al., 2005). Sodium azide was added at a final concentration of 0.04% (w/w) as a preservative.

2.3. Emulsion preparations

2.3.1. Concentrated droplet-stabilised emulsion preparations

Nano-sized primary emulsion was firstly prepared as the emulsifying agent for the droplet-stabilised emulsion. Ca-CAS dispersion (3.00 w/v % protein, 20.00 mM $CaCl_2$, pH 7.0) was mixed with soybean oil, giving 20 v/v % soy oil of the final primary emulsion. The mixture was pre-homogenized using a handheld Ultra-Turrax (IKA T10 basic, Staufen, Germany) at 30,000 rev min^{-1} for 30 s, then passes through a two-stage homogenisation (Homolab 2, FBF Italia, Italy) at pressures of 47 MPa (first stage)/5 MPa (second stage), resulting in a primary emulsion. The outlet temperature of the two-stage homogeniser was controlled by using an ice bath to avoid the heating from the high-pressure homogenisation. The pH of the primary emulsion is the same as the pH of its aqueous phase.

Primary emulsions were subsequently used as the aqueous phase to mix with the secondary oil phase (soybean oil) in volume ratio of 6:10 to prepare 16 mL of droplet-stabilised emulsion (DSE). In the final emulsion, the total oil volume fraction reached to 70 v/v %, in which the primary emulsion contributed 7.5 v/v % and the secondary oil phase contributed 62.5 v/v %. The secondary oil phase was added dropwise to the primary emulsion. Prior to adding the secondary oil phase, the pH of the primary emulsion was checked as 7.00 ± 0.05 and adjusted to pH 5.80 ± 0.05 for the acidic emulsion using 2 M HCl under mild magnetic stirring. Homogenisation of the concentrated DSE was performed using a handheld Ultra-Turrax (IKA T10 basic, Staufen, Germany) at 10,000 rev min^{-1} for 5 min. Sodium azide was added at a final concentration of 0.04 wt% as a preservative. Emulsions were prepared in duplicate for each pH value.

2.3.2. Concentrated CAS particle-stabilised emulsion preparation

Ca-CAS dispersion (3.00 w/v % protein, 20.00 mM $CaCl_2$, pH 7.0) mixed with soybean oil in ratio of 3:7 to prepare the 16 mL of high concentrated Ca-CAS particle-stabilised emulsion (PSE). Prior to adding the oil phase, the pH of the Ca-CAS dispersion was checked as 7.00 ± 0.05 or adjusted to pH 5.80 ± 0.05 for the acidic emulsion using 2 M HCl

under mild magnetic stirring. Homogenisation of the concentrated PSE was performed using a handheld Ultra-Turrax (IKA T10 basic, Staufen, Germany) at 10,000 rev min^{-1} for 5 min. Sodium azide was added at a final concentration of 0.04 wt% as a preservative. Emulsions were prepared in duplicate for each pH value.

2.4. Emulsion stability during storage and heat treatment

All emulsion samples were stored in temperature-controlled lab (22 °C) at dark place for aging. Freshly prepared emulsions are divided into portions and transfer to different vials for 0, 7, 14 and 30 days of aging to avoid repeated sampling interfering with the rheological properties of samples aged for a longer period. The bottle caps were tightened and sealed with parafilm (PARAFILM® M) to prevent moisture loss.

2.5. Particle size measurement

The *z*-average hydrodynamic diameter Ca-CAS were measured by dynamic light scattering (DLS) at 20 °C using a ZetaSizer Ultra (Malvern Instruments Ltd, Malvern, UK). The instrument used a backscattering configuration with detection at a scattering angle of 173° using an avalanche photodiode and a helium-neon laser at $\lambda = 633$ nm; refractive indices of 1.50 and 1.33 were used for protein and water, respectively.

The droplet size of emulsions with and without sodium dodecyl sulphate (SDS) was determined by static light scattering using (SLS) using a Malvern MasterSizer 2000 (Malvern Instruments Ltd, Malvern, UK). Emulsion in the absence of SDS was directly added into the MasterSizer dispersion tank under stirring at 2500 rpm during measurements. The size of individual droplets was obtained by dispersing the emulsion in 2 wt % SDS solution at volume ratio of 1:10 before SLS measurements, because SDS is capable of disrupting hydrophobic interactions and displacing protein molecules and the protein-coated droplets from the oil–water interface without changing the oil droplet size (Cheng et al., 2019, 2022a; Dickinson & Ritzoulis, 2000; Mackie et al., 2000; Tomas et al., 1994).

The refractive index of soy oil was 1.47 and water (the dispersing medium) was 1.33. Droplet size measurements are reported as De Broukere mean ($d_{4,3}$). Mean particle diameters were calculated as the average of duplicate measurements.

2.6. Zeta-potential measurements

The zeta-potentials of Ca-CAS particles, and associated emulsions, were determined by DLS at 20 °C using a ZetaSizer Ultra instrument (Malvern Instruments Ltd, Malvern, UK). The dispersions of Ca-CAS were measured at pH 7.0 and 5.8; the Ca-CAS coated primary emulsion was diluted 100 times with 20 mM $CaCl_2$ buffer before measurements to avoid multiple scattering effects. The pH of the diluted emulsions was adjusted to 7.0 and 5.8 using 0.1 M NaOH or 0.1 M HCl.

2.7. Characterisations of rheological properties

The rheological characterisations of the emulsions were conducted using AR-G2 stress-controlled rheometer (TA Instruments, Crawley, West Sussex, UK) equipped with a stainless-steel plate and plate geometry (40 mm diameter) set to a gap of 1.0 mm. The sample for rheological characterisations was transferred by a flat end stainless-steel spatula from a sample vial to the rheometer's bottom plate set at 25 °C. The geometry plate was lowered to the gap position of 1 mm. Excess emulsion was carefully trimmed out and a thin layer of mineral oil was used to seal the edge of the geometry to prevent water evaporation during the measurement. All the samples were relaxed on the rheometer following a time-sweep for 60 min at 25 °C with constant strain amplitude of 1% and constant frequency of 1 Hz before further rheological characterisations.

To measure the rheological properties of the emulsion storage at different times, a range of oscillatory experiment were performed at 25 °C: (1) the frequency sweep measurement was carried out at a constant strain of 1% for frequencies ranging from 10^{-2} Hz–10^{2} Hz; (2) the strain sweep measurement was performed at a constant frequency of 1 Hz for strain amplitude ranging from 10^{-1}%–10^{3}%.

The rheological properties of freshly prepared emulsion with heat-treatment were characterised as well. After time sweep measurements, a temperature sweep measurement was performed at fixed strain of 1% and fixed frequency of 1 Hz with four stages: (1) temperature was increased from 20 to 80 °C with a heating rate of 1 °C/min; (2) held at 80 °C for 30 min; (3) cooled from 80 to 20 °C with a cooling rate of 1 °C/min; and (4) held at 20 °C for 15 min. After that, the frequency-sweep and strain-sweep were performed as described above.

2.8. Confocal laser scanning microscopy (CLSM)

The microstructures of the emulsions were examined using a confocal laser scanning microscope (Leica, Heidelberg, Germany) equipped with a 40 × magnification oil immersion lens. Fast green and Nile red powder were added to the protein dispersion and soy oil at concentration of 0.05 mg/mL prior to emulsification. The stained emulsion was transferred onto a concave confocal microscope slide with a coverslip. Fast green was excited by a helium–neon laser at 633 nm and the emission between 638 and 750 nm was measured. Nile Red was excited by an argon laser at 488 nm and the emitted fluorescence between 494 and 605 nm was measured. To enhance image quality, sequential scanning was used. Images were captured with LAS AF software (version 2.7.3.9723) at room temperature. They were analysed using ImageJ software (ImageJ, National Institutes of Health, Bethesda, MD, USA).

2.9. Statistical analysis

Each experiment was performed in duplicate using freshly prepared samples. The results are reported as the means and standard deviations. Independent sample T-test of variance were used to compare samples in the SPSS 19.0 package (IBM, Armonk, NY, USA). The significant difference was set at a *P*-level of 0.05.

3. Results and discussion

3.1. Formation of DSE concentrated emulsions

Ca-CAS or nano-sized primary emulsions coated with Ca-CAS were used as emulsifying agents to stabilise the concentrated emulsions in the present study. The particle size and zeta-potential of Ca-CAS and primary emulsions are shown in Fig. 1a. Size distributions of Ca-CAS dispersions and the primary emulsions were monomodal at both pH conditions as shown in Fig. 1b. The *z*-average hydrodynamic diameter of Ca-CAS was 141 ± 3 and 110 ± 2 nm at pH 7.0 and 5.8, respectively. The Ca-CAS-coated emulsions were well dispersed at both pH conditions by the electrostatic stabilisation of the Ca-CAS layer. The average diameters, $d_{4,3,}$ of primary emulsion were 400 ± 10 nm at both pHs. The surface charges of Ca-CAS and the droplets were similar at a given pH, and the zeta-potential value was ~ −9 mV at pH 7.0 and ~ -6 mV at pH 5.8, respectively. The low net charge of Ca-CAS and its droplets was due to the binding and charge screening effect of calcium ions. (Cheng, Ye, Yang, et al., 2022; Guo et al., 2021; Ma et al., 2009; McCarthy et al., 2014; Sosa-Herrera et al., 2012; Zittle et al., 1958).

3.2. Droplet size distribution of the concentrated emulsions

The droplet size distributions of concentrated emulsions ($\varphi = 70\%$) stabilised by Ca-CAS (PSE) or by primary emulsion (DSE) are shown in Fig. 1c and d. The droplet size distributions of PSE at pH 7.0 and 5.8

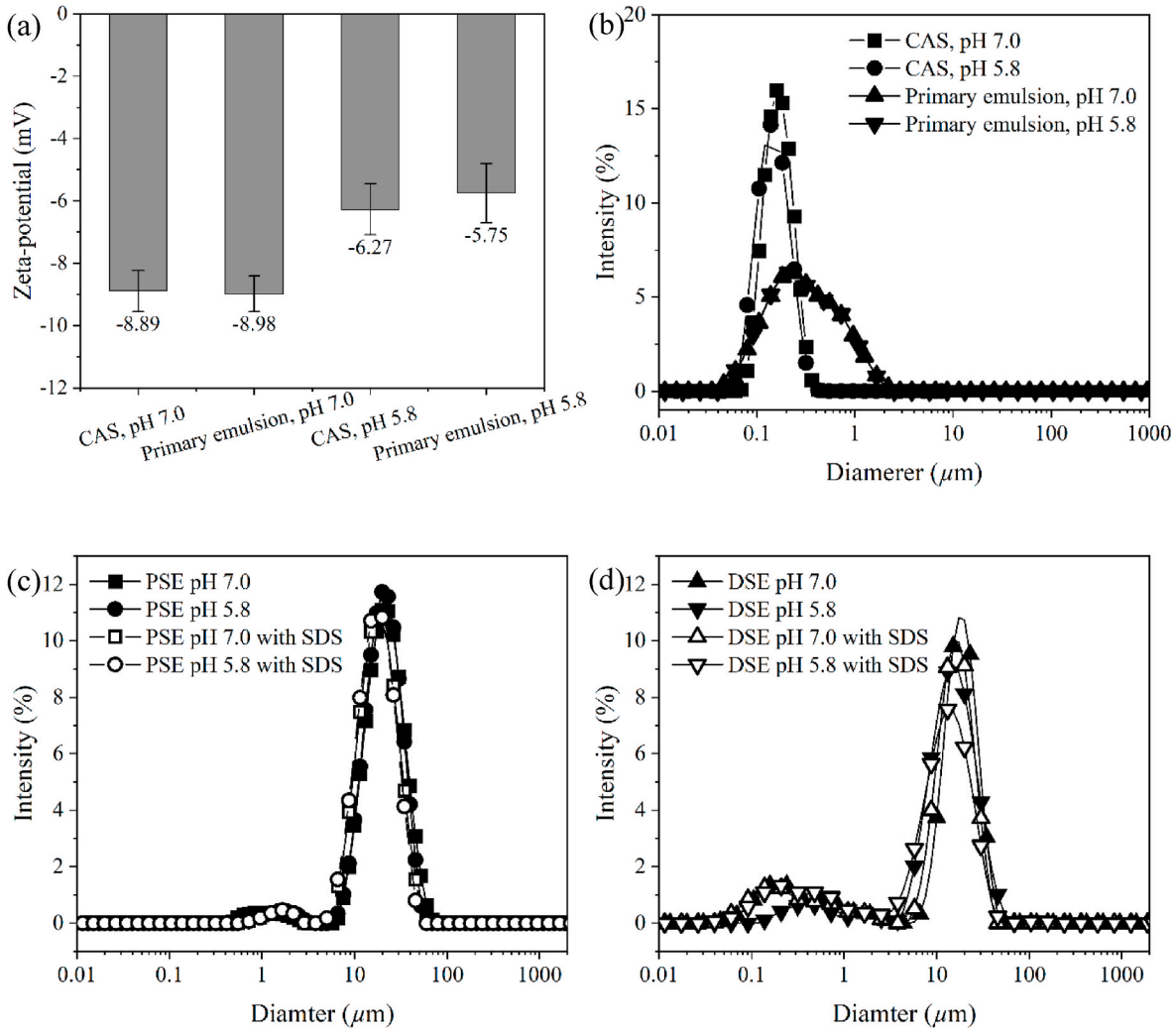

Fig. 1. (a) The zeta-potentials of Ca-CAS dispersions and Ca-CAS-stabilised nano-sized primary emulsions at pH 7.0 and 5.8; (b) particles size distributions of Ca-CAS dispersions and Ca-CAS-stabilised nano-sized primary emulsions at pH 7.0 and 5.8; (c) droplet size distributions of Ca-CAS particle stabilised-emulsion (PSE) at pH 7.0 and 5.8 in the absence and presence of SDS; (d) droplet size distributions of droplet stabilised-emulsion (DSE) at pH 7.0 and 5.8 in the absence and presence of SDS.

were similar, with a prominent peak at ~20 μm (Fig. 1c) and a polydisperse index (PDI) of 0.4. The average droplet diameters ($d_{4,3}$) for PSE at pH 7.0 and pH 5.8 were 20.06 ± 1.14 and 19.35 ± 0.36, respectively. These droplet size distributions of PSE in the absence of SDS overlapped with those in the presence of SDS, indicating that there was no droplet aggregation in the fresh PSE.

For DSE at pH 5.8, a prominent peak centred at ~20 μm was observed, with a $d_{4,3}$ of 14.12 ± 0.85 μm and PDI of 0.5 (Fig. 1d). The slightly smaller $d_{4,3}$ and larger PDI of DSE at pH 5.8 compared to PSE was due to the present of small size droplets of 0.2–2 μm. The 0.2–2 μm size droplets could be the mixture of excess primary emulsions and newly formed small size DSE. After dispersing the DSE in the SDS solution, the peak of the small sized droplet population expanded into the smaller size range and between ~0.1 and 2 μm (Fig. 1d), which corresponded to the droplet size distribution of primary emulsion only (Fig. 1b). Note also that SDS will partially disassociate the Ca-CAS particles, by supressing the hydrophobic interactions. The expansion of the peak area of small sized droplet population indicated that the adsorbed primary droplets had been detached by SDS molecules from the interface of the core droplet in DSE (Cheng et al., 2019; 2022a). This result confirmed that the primary droplets have assembled at the interface of the core droplets.

In contrast, DSE at pH 7.0 showed peaks of both the primary emulsion and the core droplets, resulting in the smaller average $d_{4,3}$ of 12.08 ± 0.12 μm and the larger PDI of 0.6 than that for DSE at pH 5.8. The droplet size distributions of the DSE at pH 7.0 with and without addition of SDS overlapped.

The average $d_{4,3}$ of DSE at pH 7.0 and 5.8 with addition of SDS was 11.89 ± 0.68 μm and 10.16 ± 1.35 μm, respectively. These results suggested that the adsorption of primary droplets at the interface of the core droplets in DSE was promoted by lowering the pH. Previous studies suggested that for casein-coating layers, bringing the pH down towards the isoelectric point (IEP = 4.6) lead to reducing the strength and range of the interlayer repulsion (Dickinson, 1999; Dickinson et al., 1997). The pH-responsive adsorption of particles have also been widely found in Pickering emulsion stabilised by different proteins or polysaccharides (Cui et al., 2022; Luo et al., 2012; Yang et al., 2007; Zhang, Holmes, et al., 2020).

3.3. Properties and stability of the concentrated emulsions

As showed in Fig. 2a-d-1, all emulsions exhibited a good stability without phase separation or oiling-off over 30 days. Except for the fresh DSE at pH 7.0 (Figs. 2c-1), the other three fresh emulsions did not flow when the glass vials were inverted (Figs. 2a-1, b-1, & d-1). This phenomenon indicated that the viscosity was high for PSE at pH 7.0, PSE at

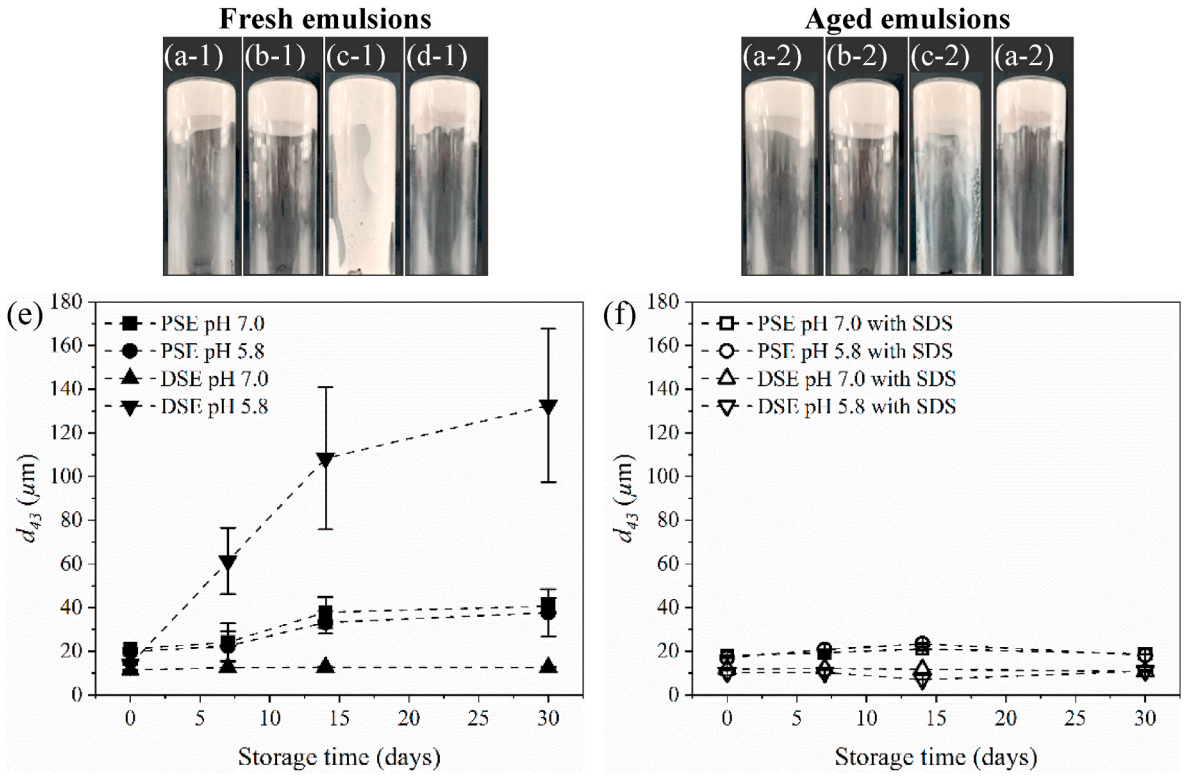

Fig. 2. Appearance of concentrated emulsion with 70% of oil volume fraction in the sealed inverted glass vails for (−1) 0 day and (−2) 30 days. Emulsion stabilised by (a) Ca-CAS at pH 7.0, (b) Ca-CAS at pH 5.8, (c) primary emulsion at pH 7.0, and (d) primary emulsion at pH 5.8. (e) The average droplet size ($d_{4,3}$) of PSE and DSE at pH 7.0 and 5.8 as a function of a storage time for 0, 7, 14 and 30 days. (f) The average droplet size ($d_{4,3}$) of PSE and DSE at pH 7.0 and 5.8 as a function of a storage time for 0, 7, 14 and 30 days in the presence of SDS.

5.8 and DSE at pH 5.8, but low for DSE at pH 7.0. It has been suggested that when the φ approaches or exceeds a critical value of φ_{max}, droplets are caged by their neighbouring droplets and do not flow, the emulsion thereby transition from a viscous liquid to a viscoelastic material (Mason, 1999). The φ_{max} has been well-established as 0.74 for the undeformable spheres with a narrow PDI of 0.1 reaching the hexagonal packing (Mason, 1999; Scott & Kilgour, 1969). However, in a polydisperse emulsion, the φ_{max} can be greater than 0.74 because the small droplets can fill the interstitial space between the large droplets (Lubachevsky & Stillinger, 1990; Scott & Kilgour, 1969; Tadros, 1994). Hence, PSEs were more solid-like than DSEs at pH 7.0 because they did not contain the primary emulsion droplet and were less polydisperse. However, DSE at pH 5.8 had also appeared to be a solid-like emulsion although it contains some amount of the primary emulsion droplets. This result indicated that other mechanisms might play a role in controlling the rheological properties. The effective volume fraction of the DSE at pH 5.8 was different from that of DSE at pH 7.0 due to the interfacial layer formed by adsorbed primary emulsion. This possible mechanism will be further discussed in the later section in combination with the results of microstructural and rheological tests.

After aging for 30 days, all emulsions did not flow when the glass vails were inverted (Fig. 2a-d-2). To examine the droplet-droplet interactions, the size of the emulsions at different storage times were measured. Except for DSE at pH 7.0, the rest of the emulsions showed an increase in size with storage time, and the droplet flocs in the aged emulsions did not dissociate during the MasterSizer measurements, as shown in Fig. 2e. After dispersing the aged emulsion in SDS solution, the droplet flocs disassociated into the individual droplets of similar size to the fresh droplets (Fig. 2f). These results suggested that (1) all types of emulsions were stable towards droplet coalescence for 30 days; (2) irreversible flocculation or aggregation of droplets developed with time because they were not dissociated during MasterSizer measurements in the absence of SDS, except for DSE at pH 7.0; (3) DSE at pH 7.0 did not flow after aging, which could be due to a depletion flocculation caused by excessive primary emulsion droplets in the aqueous phase; the depletion flocculation was not detectable by particle sizing with SLS.

3.4. Microstructure of concentrated emulsions during aging

CLSM images showed that freshly prepared emulsions had large size droplets of ~15 μm in diameter packed closely and distributed uniformly throughout the field of view (Fig. 3a-d-1). With increasing storage time, the size of individual droplets did not appear to change significantly for all the emulsions (Fig. 3a-d-2&3). These results indicated that droplets stabilised with Ca-CAS or Ca-CAS-coated primary droplets were stable against coalescence over 30 days. The signal in the aqueous phase of PSE suggested the existence of an excess proteins (Fig. 3a and b), while in the aqueous phase of DSE at pH 7.0 suggested the existence of non-adsorbed Ca-CAS-coated droplets (Fig. 3c). In contrast, the signal in the continuous phase of DSE at pH 5.8 appeared to be heterogeneous with bright patches and dark areas, indicating that the most primary droplets adsorbed onto the interface of the core droplets. Such a thick interfacial layer consisting of nano-sized primary droplets was observed for all the DSEs at pH 5.8 at different storage times (Fig. 3d). The difference between the aqueous phase of DSE at pH 7.0 and 5.8 suggested that the adsorption of primary emulsion at the interface was affected by the pH, hence the interfacial composition of the core droplets may not be the same for DSE at pH 7.0 and 5.8. At pH 7.0, the adsorption of primary droplet onto the core droplet interface might be influenced by the remaining free protein molecules in the aqueous phase. In this case, the interfacial layer of the DSE at pH 7.0 could consist of mainly proteins and a few of primary droplets. At pH 5.8, the free protein molecules in the aqueous phase tended to aggregate as particles or onto the interfaces of primary droplets, thus there was

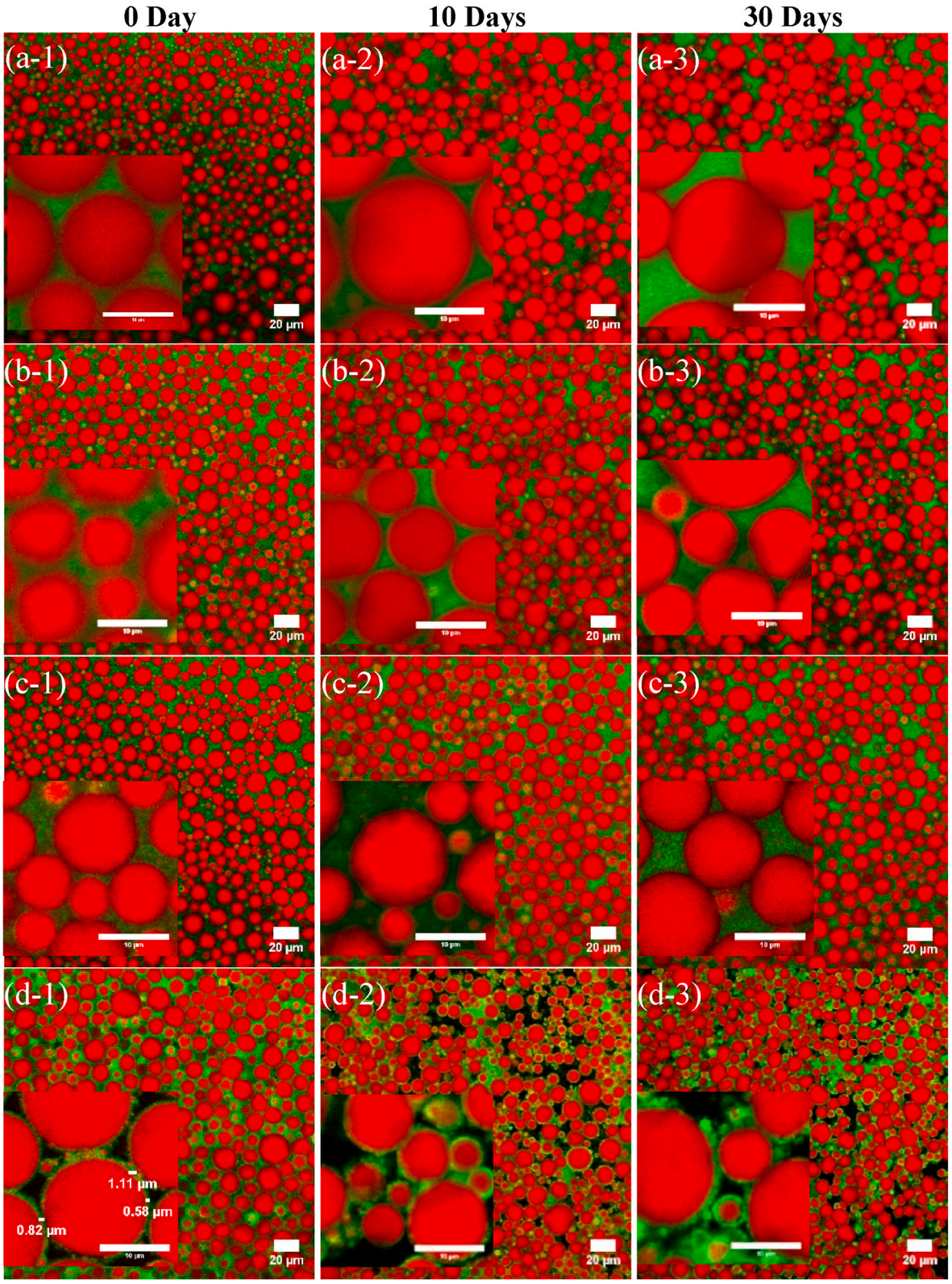

Fig. 3. 63 × Magnification confocal images of concentrated emulsion with 70% of oil volume fraction: (a) PSE at pH 7.0, (b) PSE at pH 5.8, (c) DSE at pH 7.0, and (d) DSE at pH 5.8 for (−1) 0, (−2) 10 and (−3) 30 days aging. Red colour represents the oil phase stained by Nile red and green colour represents the protein stained by fast green. Scale bar is 20 μm. Insets are associated zoom-in images with scale bar of 10 μm.

much less competition with the primary droplets in terms of the adsorption onto the core droplet interface. Hence, the interfacial layer of the DSE at pH 5.8 consisted of the primary droplets.

3.5. Viscoelasticity of concentrated DSE emulsions during aging

The frequency sweep test was performed at a fixed strain of 1%, the strain was well within the linear viscoelastic region (LVR) as shown in

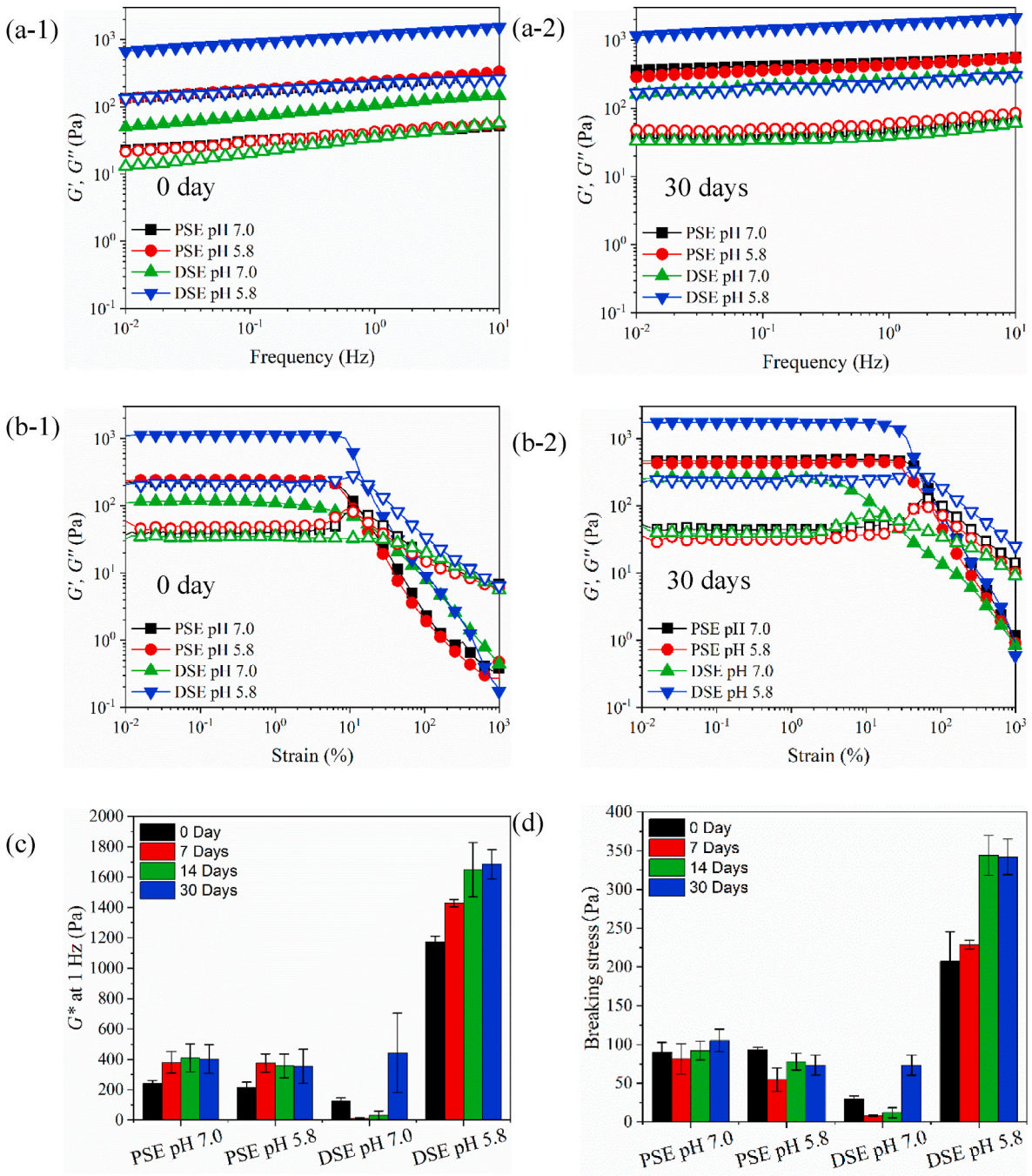

Fig. 4. G' (solid symbols) and G'' (open symbols) as (a) a function of frequency and (b) as a function of the strain for concentrated emulsion PSE (stabilised by Ca-CAS) and DSE (stabilised by primary emulsion) at pH 5.8 and pH 7.0 at (−1) 0 day and (−2) 30 days aging. (c) Complex modulus G^* (1 Hz) and (d) breaking stress of PSE and DSE at pH 7.0 and 5.8 as the function of aging time.

Fig. 4b-1&-2. The dependence of storage modulus (G') and loss modulus (G'') with frequency for 0 day and 30 days was plotted in Figs. 4a–1&-2, respectively. For the whole frequency range, both G' and G'' of all emulsions showed a weak frequency dependence; the G' of all emulsions was in parallel with and about 9 times higher than the G'', which suggested that these emulsions were weak gels before and after aging (Gabriele et al., 2001; Ross-Murphy et al., 1993). Similar dynamic weak gel characteristic had been reported for many high internal phase Pickering emulsions stabilised by food-grade particles, such as transglutaminase cross-linked gelatine (Du et al., 2021), casein and casein-hemp protein particles (Chuang et al., 2020), and soy protein/cellulose nanofibrils (Zhang, Luo, et al., 2020). The frequency dependence of aging emulsion decreased (Figs. 4a-2), indicating that inter-droplet motion was reduced after 30 days (Tang & Ghosh, 2021).

To better compare the viscoelasticity of various emulsions at different aging times, the complex modulus G^* at 1 Hz of emulsions was summarized in Fig. 4c and Table 1, where $G^* = (G'^2 + G''^2)^{1/2}$ combining the contribution from both G' and G''. In freshly prepared emulsions, the values of G^* for the PSE at both pH 7.0 (238 ± 15 Pa) and 5.8 (215 ± 25 Pa) were not significantly different. As expected, the fresh DSE showed the lowest G^* (126 ± 15 Pa) at pH 7.0 due to the high polydispersity, but the highest G^* (1174 ± 28 Pa) at pH 5.8. The high G^* in the fresh DSE at pH 5.8 than other emulsions ($P > 0.05$) could suggest that there were DSE droplet-droplet networking through the primary droplets that were

Table 1
Complex moduli G* at 1 Hz (Pa) of PSE and DSE at pH 7.0 and 5.8 after 0 day, 30 days aging, and heating at 80 °C for 30 min.

	G^* at 1 Hz (Pa)		
	0 D	30 D	80 °C
PSE, pH 7.0	238 ± 21^{Aa}	403 ± 68^{Ba}	583 ± 76^{Ca}
PSE, pH 5.8	215 ± 35^{Aa}	354 ± 79^{Ba}	653 ± 20^{Ca}
DSE, pH 7.0	126 ± 21^{Ab}	443 ± 127^{Ba}	1312 ± 205^{Cb}
DSE, pH 5.8	1174 ± 39^{Ac}	1685 ± 68^{Bb}	1801 ± 69^{Bc}

Different letters in capitals represent significant differences between different storage time and temperature of the same sample according to SPSS T-test ($P < 0.05$); different letters in lower case represent significant differences between samples at same storage time and temperature. Experimental data are the means of duplicate samples. Numbers in parentheses represent the standard error from duplicates.

entrapped within two interfaces.

Another possible contributor for the high G^* of DSE at pH 5.8 was the thick interfacial layer for DSE at pH 5.8, which resulted in an increase in the effective volume fraction of the emulsion. When taking a thickness of the interfacial layer, h, into account, the effective volume fraction, φ_{eff} can be calculated using **equation (1)** (Mason, 1999):

$$\varphi_{eff} \approx \varphi_{core}\left[1+\frac{2h}{D}\right]^3 \quad (1)$$

where φ_{core} is oil volume fraction of the large core droplet, D is the mean droplet diameter ($D \approx 15$ μm, given by the emulsion with addition of SDS measured by SLS after excluding the contribution from small droplets), which is valid for $2h \ll d$ (Erramreddy & Ghosh, 2015; Mason, 1999; Princen et al., 1980; Wilking & Mason, 2007).

For DSE at pH 5.8, the primary droplet layer at the core droplet surface, h, was contributed to ~0.87 μm thickness as estimated by the difference in large droplet diameter before (14.59 ± 0.17 μm) and after adding SDS (12.85 ± 0.41 μm). The φ_{eff} was calculated as 0.87 which was 1.39 times higher than the set φ_{core} of 0.625 (the primary emulsion accounted for oil volume fraction of 0.075). Similar results have been reported previously that an increase of φ_{eff} by increasing the size ratio of emulsifier to the droplet has led to the dramatic increase in the elasticity of the concentrated emulsion ($\varphi = 0.3-0.9$) (Chanamai & McClements, 2000; Erramreddy & Ghosh, 2015; Hemar & Horne, 2000; Roullet et al., 2019). For DSE at pH 7.0, the difference in the large droplet size before (15.44 ± 0.29 μm) and after adding SDS (15.44 ± 0.34 μm) was not significant. The φ_{eff} of DSE at pH 7.0 should then be similar to the set φ_{core} (= 0.625) and was probably below or near to its φ_{RCP} (>0.64, due to its polydispersity).

Therefore, the highest G^* of the DSE at pH 5.8 could be attributed to the large φ_{eff} caused by the thick interfacial layer consisting of primary emulsion droplets and the droplet interactions through this thick interfacial layer, while the lowest G^* of DSE at pH 7.0 among all emulsions could be attributed to its lowest φ_{eff} and high polydispersity.

For PSE, the previous study showed that the thickness of Ca-CAS-particle layer, h, at the oil-water interfaces is ~30 nm (Cheng, Ye, Yang, et al., 2022). Taking the 2 h by Ca-CAS-particles as 0.06 μm (h = 0.03 μm), the calculated φ_{eff} was 0.71 and slightly higher than the φ_{core} of 0.7 of PSE. This result was consistent with other studies that have used nano-sized protein particles (soy β-conglycinin and ovalbumin) as emulsifier in concentrated emulsions where the thickness of the interfacial layer had a negligible effect on the viscoelasticity of the emulsion (Xu et al., 2018, 2019).

During aging, the G^* of PSE increased to ~400 Pa after 7 days at both pH values and then did not change during further storage. The G^* of DSE at pH 7.0 were 13 ± 3, 32 ± 20 and 443 ± 184 Pa for 7, 14 and 30 days, respectively, which were significantly lower or higher than that of the fresh sample. In contrast to DSE at pH 7.0, the G^* of DSE at pH 5.8 steadily increased with aging time. The G^* of DSE at pH 5.8 increased from 1174 ± 28 at fresh state to 1430 ± 18 Pa after 7 days of aging. The subsequent increase in G^* was not significant between 14 (1650 ± 127 Pa) and 30 days (1686 ± 68 Pa) of aging. The trend of the increase in G^* was similar between DSE at pH 5.8 and PSE at both pH values, suggesting that the three emulsions may follow the same mechanism of restructuring during aging. The fluctuation of G^* from DSE at pH 7.0 was possibly a result from the weak and inhomogeneous spatial structure during aging for 0–14 days which formed a stable network after 30 days.

A possible mechanism accounting for the increase in G^* of emulsion during storage could be the gravity-driven microphase separation and protein-protein aggregation in order to reduce the Gibbs free energy in the emulsion (Tadros, 2004). Tadros (2004) suggested that the contraction of the droplet network during the storage could be driven by gravity force if the droplet size is larger than 1 μm, resulting in phase separation. Between the close contact droplets, the droplet-droplet aggregation might occur, resulting in irreversible increase in droplet size as shown in SLS measurements Fig. 2e. Due to the low zeta potential (6–9 mV absolute) and high electrolyte concentration (20 mM $CaCl_2$) in these emulsions, irreversible aggregation between the adsorbed proteins may be caused by calcium ion cross-linking, electrostatic and/or hydrophobic interactions. Nevertheless, the positive relationship between the droplet flocculation and the G' of emulsions with storage time has been previously reported; this is because the droplet clusters with the entrapped aqueous phase enhance the effective volume fraction of emulsion, resulting in a greater G' (Anton et al., 2001; Hayati et al., 2007; Tadros, 2004). In addition to the gravity, depletion flocculation induced by the excess non-adsorbed primary emulsion droplets may also play a role in contributing to the microphase separation and a greater G^* after 30 days (Aben et al., 2012; Dickinson & Golding, 1997a, 1997b).

The stability of emulsion under the large deformation oscillation is shown in Figs. 4b–1&-2, in which G' and G'' were plotted against the applied strain amplitude at a fixed frequency of 1 Hz. Within the LVR, all emulsions exhibited a gel-like behaviour, in which G' was higher than G'', with both G' and G'' being independent of the applied strain until a certain critical strain point. The critical strain point could be defined as both G' and G'' started to deviate from the LVR, which suggested that the sample started to flow. For fresh emulsions (Figs. 4b-1), the maximum strain of the LVR was in the order DSE at pH 5.8 (9.95 ± 0.16%) > PSE at both pH (7.34 ± 1.00%) > DSE at pH 7.0 (1.60 ± 0.00%). After 30 days (Figs. 4b-2), the maximum strain of the LVR of all emulsions was increased as DSE at pH 5.8 (25.57 ± 0.79%) ≈ PSE at both pH (25.55 ± 0.12%) > DSE at pH 7.0 (4.55 ± 0.48%). Compared to the other three emulsions, DSE at pH 7.0 had a weaker inter-droplet interaction at a given storage time that was attributed to its broad distribution and low φ_{eff}.

3.6. Stability and viscoelasticity of concentrated emulsions against heating

After heating at 80 °C for 30 min, all the freshly made concentrated emulsions gelled, without phase separation, and did not flow when the glass vials were inverted (Fig. 5a–d). The droplet size of heated emulsions in the absence or the presence of SDS is shown in Fig. 5e and f. There was no significant difference (P > 0.05) in the size of emulsion droplets both in the presence and the absence of SDS before and after heating. This result indicated that emulsions coated with Ca-CAS layer or primary droplet layer were stable against coalescence during heating.

The microstructures of the heated emulsion observed by CLSM are shown in Fig. 5g–j. As shown in the confocal images, the size of the core droplets after heating remained similar to the size of the fresh emulsion (Fig. 3a-d-1), confirming that there was no droplet coalescence of core droplets stabilised by either the Ca-CAS layer or primary droplet layer during heating process.

For PSE after heating, the droplet network was consisted of the protein-rich and protein-poor regions (Fig. 3g and h, insets). In the protein-rich region, two droplet interfaces were connected by protein

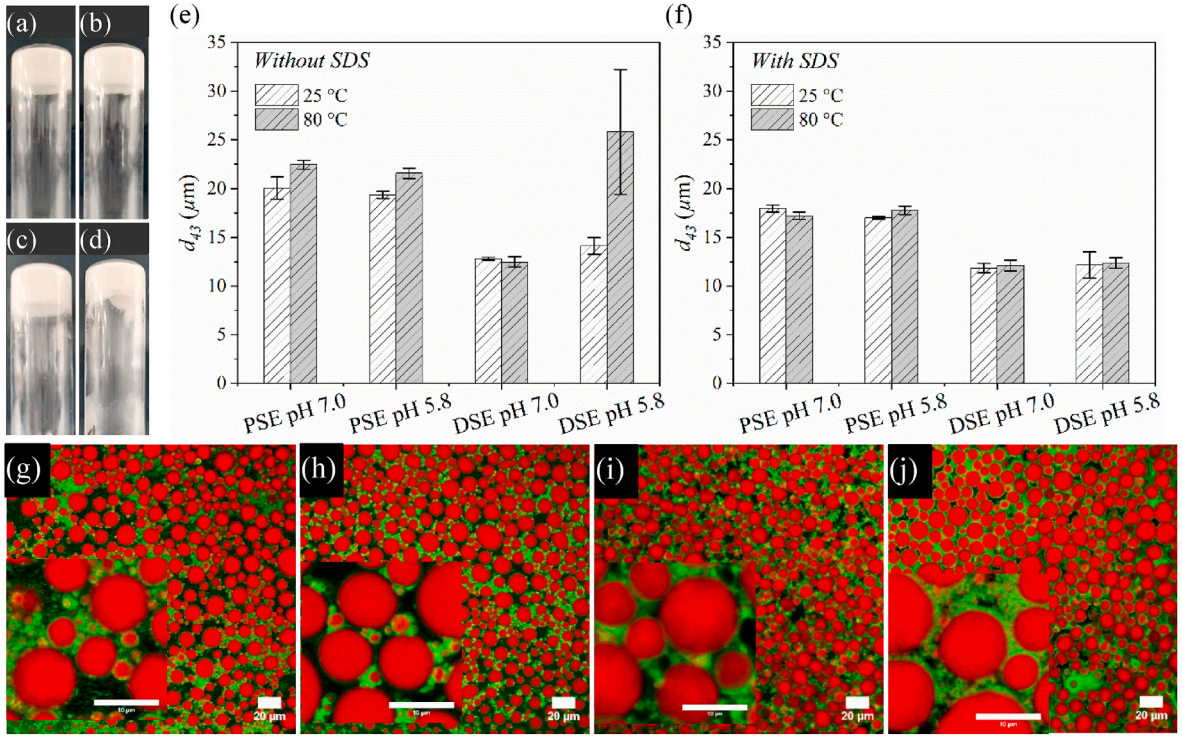

Fig. 5. Appearance (left panel) of 70% concentrated emulsions stabilised by (a) Ca-CAS at pH 7.0, (b) Ca-CAS at pH 5.8, (c) primary emulsion at pH 7.0, and (d) primary emulsion at pH 5.8 in the inverted seal glass vails after heating in oven at 80 °C for 30 min. The average droplet size ($d_{4,3}$) of PSE and DSE at pH 7.0 and 5.8 before and after heating (e) with the absence of SDS and (f) with the presence of SDS. 63 × Magnification confocal images of concentrated emulsion that stabilised by (g) Ca-CAS at pH 7.0, (h) Ca-CAS at pH 5.8, (i) primary emulsion droplets at pH 7.0, and (j) primary emulsion droplets at pH 5.8 after heating. Scale bar is 20 μm. Insets are associated zoom-in images with scale bar of 10 μm.

aggregates, or in another words, the protein aggregates were entrapped among the droplets. In the protein-poor region, interfaces of the droplets lacked protein signals because these areas were covered by small size protein particles. Some of the droplet network of PSE was disconnected in the protein-poor region due to the lack of the large protein aggregates to fill the gaps between the droplets. In contrast, the network of DSE was continuous and tight. The core droplets were embedded in the matrix and were made up of aggregated primary droplets (Fig. 5i and j, insets).

The changes in the elasticity of the emulsions with the heating temperature were monitored by the temperature ramp (Fig. 6a, inset). The rapid increase in G' with the increasing temperature indicated that the emulsion converted into an emulsion gel. The rapid increase in G' in all the emulsions started at ~40 °C, which was consistent with the previously reported gelation temperature (~40 °C) of caseinate-stabilised emulsions or casein micelles solutions in the presence of Ca^{2+} (Balakrishnan et al., 2018; Dickinson & Casanova, 1999; McCarthy et al., 2014). When the temperature arrived to 80 °C, the G' of all emulsion gels reached a plateau level over the time sweep at 80 °C for 30 min. The stable G' of the emulsion over the holding time confirmed that the structure of emulsion gels resisted to heat-induced destabilization, such as droplet coalescence, phase separation or syneresis. The gel strength further increased during the cooling step, which was possibly attributed to the increase in the strength of hydrogen bonds at low temperatures (Cordier & Grzesiek, 2002).

The subsequent frequency-dependent G' and G'' of PSE and DSE is plotted in Fig. 6a. The weak frequency dependence of both G' and G'' suggested that all the heated emulsions were weak gels (Gabriele et al., 2001; Ross-Murphy et al., 1993). As compared to the unheated emulsion (Figs. 4a-1), the frequency dependence of the heated emulsion was less pronounced (Fig. 6a) (Tang & Ghosh, 2021). This result was consistent with the observations that all emulsions did not flow in the inverted tube after heating (Fig. 5a–d) and the droplets were bridged together after heating (Fig. 5g–j).

The gel strength of unheated emulsion and heated emulsions was represented by the complex modulus G^* at 1 Hz as presented in Fig. 6b and Table 1. The G^* of the emulsion was significantly increased after heat-treatment compared to that of the unheated emulsions. The gel strength of heated PSE did not show a significant dependency on the pH, whereas the gel strength of heated DSE did (Table 1).

The large deformation rheological properties of heat-induced emulsion gels were measured by strain sweep as shown in Fig. 6c, in which G' and G'' were plotted against the applied strain amplitude. All the samples exhibited a gel like behaviours in the LVR, both G' and G'' were independent of the applied strain up to the critical strain point. For all the heated emulsions, at a strain close to the critical strain point, the G'' showed the over-shoot feature, indicating the presence of droplet compression in the heated emulsion causing the high energy dissipation before the breakdown of network (Seth et al., 2011).

The breaking stress of the unheated and heated emulsions was summarized in Fig. 6d. As shown in Fig. 6d, the breaking stress of emulsion was significantly increased by the heat-treatment, indicating that the heated emulsions had a higher stability towards large deformation than the unheated emulsions. The breaking stress of emulsions shared a similar trend to their G^* suggesting their large deformation behaviour correlated well with the small deformation viscoelastic behaviour. It was clear that the greater average G^* and breaking stress in heated emulsions resulted from the heated-induced protein-protein aggregation (Fig. 5g–j) and droplet flocculation (Fig. 5e and f). Since the heat-induced interactions were superimposed on the droplet interactions provided by the adsorbed primary droplet layer, the G^* and breaking stress of DSE at pH 5.8 were significantly higher than that at pH 7.0.

4. Conclusions

In this study, Ca-CAS particles and Ca-CAS coated nano-sized

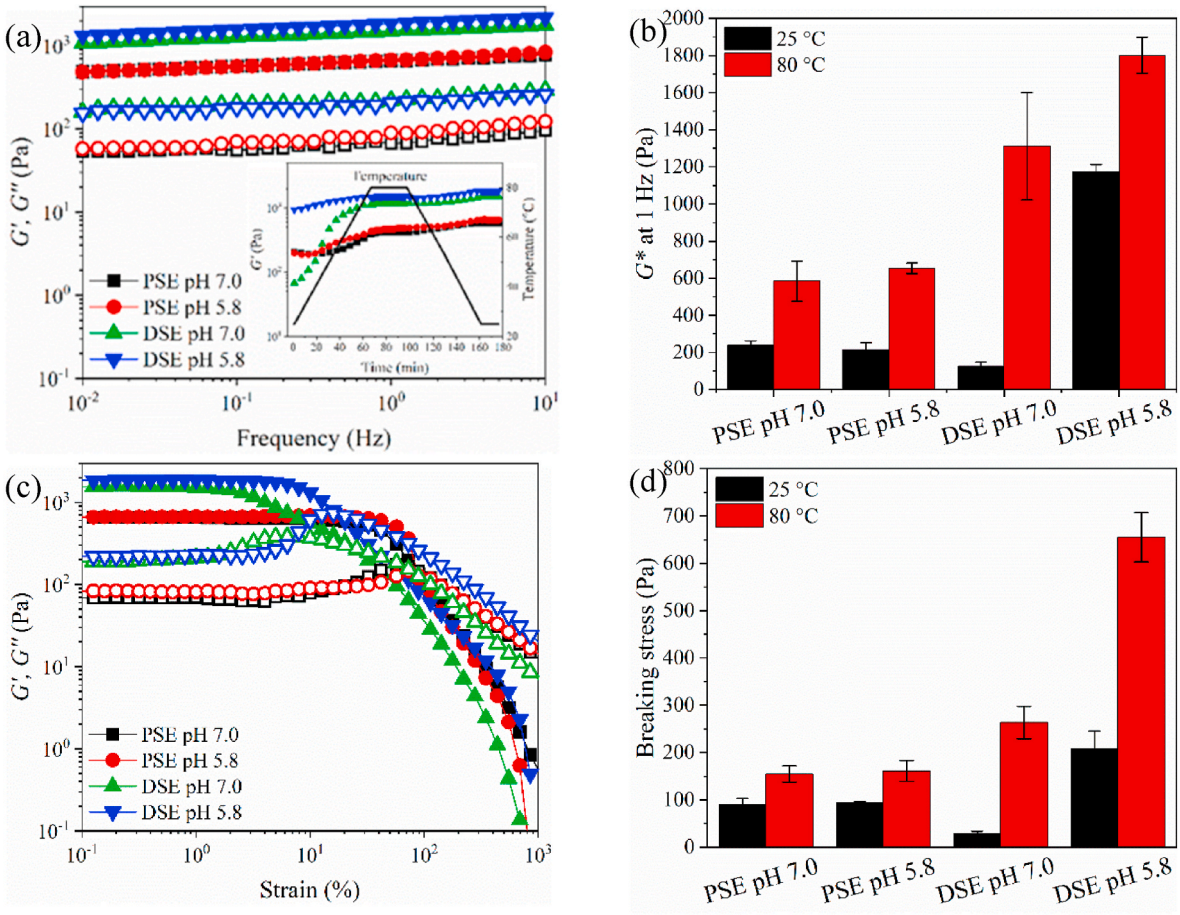

Fig. 6. (a) The frequency dependence and (c) strain amplitude behaviour of G' (solid symbols) and G'' (open symbols) for concentrated emulsion stabilised by Ca-CAS and primary emulsion at pH 5.8 and pH 7.0 after heating at 80 °C for 30 min. (b) The complex moduli G^* (1 Hz) and (d) breaking stress for PSE and DSE at pH 7.0 and 5.8 as the function of temperature at 25 and 80 °C.

primary emulsions exhibited good emulsifying agents in the preparation of 70% oil-in-water emulsion. The viscoelasticity of the concentrated emulsion stabilised by Ca-CAS (PSE) was insensitive to pH in the range between 7.0 and 5.8. When the primary emulsion was used as the emulsifier to stabilise emulsion (DSE), the viscoelasticity of the concentrated emulsion was altered. The thick droplet layer at the surface of the core droplet in DSE formed at pH 5.8 increased the effective volume fraction of the core droplet phase by a factor of 1.39, whereas the Ca-CAS layer of PSE increased the effective volume fraction of the core droplet phase by a factor of 1.01, leading to a ~6-fold higher viscoelasticity of DSE compared to PSE in the fresh state.

After the long-term storage (30 days) and heat-treatment (80 °C for 30 min), all concentrated emulsions showed excellent stability against droplet coalescence, and transformed into self-supporting gels. Compared to the other three emulsions, DSE at pH 5.8 exhibited the highest viscoelasticity because of the positive effects of aging and heating superimposed on its initially high viscoelasticity. The significant increase in the viscoelasticity of the aged emulsions was attributed to the gravity-driven microphase separation and droplet flocculation. The droplet flocs together with the entrapped aqueous phase led to the increase in effective volume fraction. Heating the emulsions to 80 °C led to a dramatic increase in the rheological properties with the highest viscoelasticity. With increasing temperature, the interactions between proteins increased resulting in protein aggregation between the non-adsorbed proteins themselves and/or between the non-adsorbed proteins and absorbed proteins. The contacting droplets in the concentrated emulsions were associated together through the protein aggregates or primary droplets, forming a three-dimensional droplet network. This study provided us with a clear picture of using droplet-stabilised interface in improving the mechanical strength of food-grade concentrated emulsion.

CRediT authorship contribution statement

Lirong Cheng: Conceptualisation, Methodology, Software, Validation, Investigation, Formal analysis, Data Curation, Visualization, Writing - original draft. Aiqian Ye: Conceptualisation, Resources, Funding acquisition, Supervision, Project administration, Writing - review & editing. Zhi Yang: Methodology, Writing – review & editing. Yacine Hemar: Writing - review & editing, Supervision. Harjinder Singh: Conceptualisation, Funding acquisition, Writing - review & editing, Supervision.

Declaration of competing interest

The authors have declared no conflicts of interest.

Data availability

Data will be made available on request.

Acknowledgements

This work was funded by the Riddet Institute, a National Centre of Research Excellence, and by the New Zealand Tertiary Education Commission. We also thank the Manawatu Microscopy and Imaging

Centre at Massey University for technical support.

References

Abdullah, Weiss, J., Ahmad, T., Zhang, C., & Zhang, H. (2020). A review of recent progress on high internal-phase Pickering emulsions in food science. *Trends in Food Science and Technology, 106*, 91–103. https://doi.org/10.1016/j.tifs.2020.10.016

Aben, S., Holtze, C., Tadros, T., & Schurtenberger, P. (2012). Rheological investigations on the creaming of depletion-flocculated emulsions. *Langmuir, 28*(21), 7967–7975. https://doi.org/10.1021/la300221m

Anton, M., Chapleau, N., Beaumal, V., Delépine, S., & De Lamballerie-Anton, M. (2001). Effect of high-pressure treatment on rheology of oil-in-water emulsions prepared with hen egg yolk. *Innovative Food Science and Emerging Technologies, 2*(1), 9–21. https://doi.org/10.1016/S1466-8564(00)00036-9

Balakrishnan, G., Silva, J. V. C., Nicolai, T., Chassenieux, C., Bovay, C., Buczkowski, J., & Schmitt, C. (2018). Specific effect of calcium ions on thermal gelation of aqueous micellar casein suspensions. *Colloids and Surfaces B: Biointerfaces, 163*, 218–224. https://doi.org/10.1016/j.colsurfb.2017.12.029

Barbetta, A., & Cameron, N. R. (2004). Morphology and surface area of emulsion-derived (PolyHIPE) solid foams prepared with oil-phase soluble porogenic solvents: Three-component surfactant system. *Macromolecules, 37*(9), 3202–3213. https://doi.org/10.1021/ma035944y

Berli, C. L. A. (2007). Rheology and phase behavior of aggregating emulsions related to droplet-droplet interactions. *Brazilian Journal of Chemical Engineering, 24*(2), 203–210. https://doi.org/10.1590/S0104-66322007000200005

Binks, B. P. (2002). Particles as surfactants—similarities and differences. *Current Opinion in Colloid & Interface Science, 7*(1–2), 21–41. https://doi.org/10.1016/S1359-0294(02)00008-0

Cameron, N. R., & Sherrington, D. C. (1996). High internal phase emulsions (HIPEs) — structure, properties and use in polymer preparation. *Advances in Polymer Science, 126*, 163–214. https://doi.org/10.1007/3-540-60484-7_4

Chanamai, R., & McClements, D. J. (2000). Dependence of creaming and rheology of monodisperse oil-in-water emulsions on droplet size and concentration. *Colloids and Surfaces A: Physicochemical and Engineering Aspects, 172*(1–3), 79–86. https://doi.org/10.1016/S0927-7757(00)00551-3

Cheng, L., Ye, A., Hemar, Y., Gilbert, E. P., de Campo, L., Whitten, A. E., & Singh, H. (2019). Interfacial structures of droplet-stabilized emulsions formed with whey protein microgel particles as revealed by small- and ultra-small-angle neutron scattering. *Langmuir, 35*(37), 12017–12027. https://doi.org/10.1021/acs.langmuir.9b01966

Cheng, L., Ye, A., Hemar, Y., & Singh, H. (2022a). Modification of the interfacial structure of droplet-stabilised emulsions during in vitro dynamic gastric digestion: Impact on in vitro intestinal lipid digestion. *Journal of Colloid and Interface Science, 608*, 1286–1296. https://doi.org/10.1016/j.jcis.2021.10.075

Cheng, L., Ye, A., Yang, Z., Gilbert, E. P., Knott, R., de Campo, L., Storer, B., Hemar, Y., & Singh, H. (2022b). Small-angle X-ray scattering (SAXS) and small-angle neutron scattering (SANS) study on the structure of sodium caseinate in dispersions and at the oil-water interface: Effect of calcium ions. *Food Structure, 32*, Article 100276. https://doi.org/10.1016/j.foostr.2022.100276

Chuang, C., Ye, A., Anema, S. G., & Loveday, S. M. (2020). Concentrated pickering emulsions stabilised by hemp globulin–caseinate nanoparticles: Tuning the rheological properties by adjusting the hemp globulin : Caseinate ratio. *Food & Function, 11*(11), 10193–10204. https://doi.org/10.1039/D0FO01745K

Cordier, F., & Grzesiek, S. (2002). Temperature-dependence of protein hydrogen bond properties as studied by high-resolution NMR. *Journal of Molecular Biology, 317*(5), 739–752. https://doi.org/10.1006/jmbi.2002.5446

Cui, F., McClements, D. J., Liu, X., Liu, F., & Ngai, T. (2022). Development of pH-responsive emulsions stabilized by whey protein fibrils. *Food Hydrocolloids, 122*, Article 107067. https://doi.org/10.1016/j.foodhyd.2021.107067

Desmond, K. W., & Weeks, E. R. (2014). Influence of particle size distribution on random close packing of spheres. *Physical Review E, 90*(2), Article 022204. https://doi.org/10.1103/PhysRevE.90.022204

Dickinson, E. (1999). Adsorbed protein layers at fluid interfaces: Interactions, structure and surface rheology. *Colloids and Surfaces B: Biointerfaces, 15*(2), 161–176. https://doi.org/10.1016/S0927-7765(99)00042-9

Dickinson, E., & Casanova, H. (1999). A thermoreversible emulsion gel based on sodium caseinate. *Food Hydrocolloids, 13*(4), 285–289. https://doi.org/10.1016/S0268-005X(99)00010-7

Dickinson, E., & Golding, M. (1997a). Depletion flocculation of emulsions containing unadsorbed sodium caseinate. *Food Hydrocolloids, 11*(1), 13–18. https://doi.org/10.1016/S0268-005X(97)80005-7

Dickinson, E., & Golding, M. (1997b). Rheology of sodium caseinate stabilized oil-in-water emulsions. *Journal of Colloid and Interface Science, 191*(1), 166–176. https://doi.org/10.1006/jcis.1997.5221

Dickinson, E., Pinfield, V. J., Horne, D. S., & Leermakers, F. A. M. (1997). Self-consistent-field modelling of adsorbed casein: Interaction between two protein-coated surfaces. *Journal of the Chemical Society, Faraday Transactions, 93*(9), 1785–1790. https://doi.org/10.1039/a608417f

Dickinson, E., & Ritzoulis, C. (2000). Creaming and rheology of oil-in-water emulsions containing sodium dodecyl sulfate and sodium caseinate. *Journal of Colloid and Interface Science, 224*(1), 148–154. https://doi.org/10.1006/jcis.1999.6682

Dimitrova, T. D., & Leal-Calderon, F. (2004). Rheological properties of highly concentrated protein-stabilized emulsions. *Advances in Colloid and Interface Science, 108*(109), 49–61. https://doi.org/10.1016/j.cis.2003.10.002

Du, J., Dai, H., Wang, H., Yu, Y., Zhu, H., Fu, Y., Ma, L., Peng, L., Li, L., Wang, Q., & Zhang, Y. (2021). Preparation of high thermal stability gelatin emulsion and its application in 3D printing. *Food Hydrocolloids, 113*, Article 106536. https://doi.org/10.1016/j.foodhyd.2020.106536

Erramreddy, V. V., & Ghosh, S. (2015). Influence of droplet size on repulsive and attractive nanoemulsion gelation. *Colloids and Surfaces A: Physicochemical and Engineering Aspects, 484*, 144–152. https://doi.org/10.1016/j.colsurfa.2015.07.027

Foudazi, R., Masalova, I., & Malkin, A. Y. (2012). The rheology of binary mixtures of highly concentrated emulsions: Effect of droplet size ratio. *Journal of Rheology, 56*(5), 1299. https://doi.org/10.1122/1.4736556

Gabriele, D., de Cindio, B., & D'Antona, P. (2001). A weak gel model for foods. *Rheologica Acta, 40*(2), 120–127. https://doi.org/10.1007/s003970000139

Geremias-Andrade, I. M., Souki, N. P. D. B. G., Moraes, I. C. F., & Pinho, S. C. (2017). Rheological and mechanical characterization of curcumin-loaded emulsion-filled gels produced with whey protein isolate and xanthan gum. *Lebensmittel-Wissenschaft & Technologie, 86*, 166–173. https://doi.org/10.1016/j.lwt.2017.07.063

Guo, Y., Wu, C., Du, M., Lin, S., Xu, X., & Yu, P. (2021). In-situ dispersion of casein to form nanoparticles for Pickering high internal phase emulsions. *Lebensmittel-Wissenschaft & Technologie, 139*(1), Article 110538. https://doi.org/10.1016/j.lwt.2020.110538

Hayati, I. N., Che Man, Y. B., Tan, C. P., & Aini, I. N. (2007). Stability and rheology of concentrated O/W emulsions based on soybean oil/palm kernel olein blends. *Food Research International, 40*(8), 1051–1061. https://doi.org/10.1016/j.foodres.2007.05.008

Hemar, Y., & Horne, D. S. (2000). Dynamic rheological properties of highly concentrated protein-stabilized emulsions. *Langmuir, 16*(7), 3050–3057. https://doi.org/10.1021/la9908440

Huang, X.-N., Zhu, J.-J., Xi, Y.-K., Yin, S.-W., Ngai, T., & Yang, X.-Q. (2019). Protein-based pickering high internal phase emulsions as nutraceutical vehicles of and the template for advanced materials: A perspective paper. *Journal of Agricultural and Food Chemistry, 67*(35), 9719–9726. https://doi.org/10.1021/acs.jafc.9b03356

Hu, Y. Q., Yin, S. W., Zhu, J. H., Qi, J. R., Guo, J., Wu, L. Y., Tang, C. H., & Yang, X. Q. (2016). Fabrication and characterization of novel Pickering emulsions and Pickering high internal emulsions stabilized by gliadin colloidal particles. *Food Hydrocolloids, 61*, 300–310. https://doi.org/10.1016/j.foodhyd.2016.05.028

Jiang, Y., Zhang, C., Yuan, J., Wu, Y., Li, F., Li, D., & Huang, Q. (2019). Effects of pectin polydispersity on zein/pectin composite nanoparticles (ZAPs) as high internal-phase Pickering emulsion stabilizers. *Carbohydrate Polymers, 219*, 77–86. https://doi.org/10.1016/j.carbpol.2019.05.025

Lacasse, M. D., Grest, G. S., Levine, D., Mason, T. G., & Weitz, D. A. (1996). Model for the elasticity of compressed emulsions. *Physical Review Letters, 76*(18), 3448–3451. https://doi.org/10.1103/PhysRevLett.76.3448

Li, Z., Dai, L., Wang, D., Mao, L., & Gao, Y. (2018). Stabilization and rheology of concentrated emulsions using the natural emulsifiers quillaja saponins and rhamnolipids. *Journal of Agricultural and Food Chemistry, 66*(15), 3922–3929. https://doi.org/10.1021/acs.jafc.7b05291

Li, X., Xianbing, X., Song, L., Bi, A., Wu, C., Ma, Y., Du, M., & Zhu, B. (2020). High internal phase emulsion for food-grade 3D printing materials. *ACS Applied Materials & Interfaces, 12*(40), 45493–45503. https://doi.org/10.1021/acsami.0c11434

Lubachevsky, B. D., & Stillinger, F. H. (1990). Geometric properties of random disk packings. *Journal of Statistical Physics, 60*(5–6), 561–583. https://doi.org/10.1007/BF01025983

Luo, Z., Murray, B. S., Ross, A. L., Povey, M. J. W., Morgan, M. R. A., & Day, A. J. (2012). Effects of pH on the ability of flavonoids to act as Pickering emulsion stabilizers. *Colloids and Surfaces B: Biointerfaces, 92*, 84–90. https://doi.org/10.1016/j.colsurfb.2011.11.027

Mackie, A. R., Gunning, A. P., Wilde, P. J., & Morris, V. J. (2000). Competitive displacement of β-lactoglobulin from the air/water interface by sodium dodecyl sulfate. *Langmuir, 16*(21), 8176–8181. https://doi.org/10.1021/la0003950

Ma, H., Forssell, P., Partanen, R., Seppänen, R., Buchert, J., & Boer, H. (2009). Sodium caseinates with an altered isoelectric point as emulsifiers in oil/water systems. *Journal of Agricultural and Food Chemistry, 57*(9), 3800–3807. https://doi.org/10.1021/jf803104s

Mason, T. G. (1999). New fundamental concepts in emulsion theology. *Current Opinion in Colloid & Interface Science, 4*(3), 231–238. https://doi.org/10.1016/S1359-0294(99)00035-7

Mason, T. G., Bibette, J., & Weitz, D. A. (1996). Yielding and flow of monodisperse emulsions. *Journal of Colloid and Interface Science, 179*(2), 439–448. https://doi.org/10.1006/jcis.1996.0235

McCarthy, N. A., Kelly, A. L., O'Mahony, J. A., & Fenelon, M. A. (2014). Sensitivity of emulsions stabilised by bovine β-casein and lactoferrin to heat and CaCl2. *Food Hydrocolloids, 35*, 420–428. https://doi.org/10.1016/j.foodhyd.2013.06.021

Murray, B. S., Dickinson, E., & Wang, Y. (2009). Food Hydrocolloids Bubble stability in the presence of oil-in-water emulsion droplets : Influence of surface shear versus dilatational rheology. *Food Hydrocolloids, 23*(4), 1198–1208. https://doi.org/10.1016/j.foodhyd.2008.07.015

Pal, R. (1996). Effect of droplet size on the rheology of emulsions. *AIChE Journal, 42*(11), 3181–3190. https://doi.org/10.1002/aic.690421119

Patel, A. R., & Dewettinck, K. (2016). Edible oil structuring: An overview and recent updates. *Food & Function, 7*(1), 20–29. https://doi.org/10.1039/C5FO01006C

Princen, H., Aronson, M., & Moser, J. (1980). Highly concentrated emulsions: II. Real systems. The effect of film thickness and contact angle on the volume fraction in creamed emulsions. *Journal of Colloid and Interface Science, 75*(1), 246–270. https://doi.org/10.1016/0021-9797(80)90367-7

Princen, H., & Kiss, A. (1986). Rheology of foams and highly concentrated emulsions. *Journal of Colloid and Interface Science, 112*(2), 427–437. https://doi.org/10.1016/0021-9797(86)90111-6

Ross-Murphy, S. B. B., Shatwell, K. P. P., Sb, R.-M., & Kp, S. (1993). Polysaccharide strong and weak gels. *Biorheology, 30*(3–4), 217–227. https://doi.org/10.3233/BIR-1993-303-407

Roullet, M., Clegg, P. S., & Frith, W. J. (2019). Viscosity of protein-stabilized emulsions: Contributions of components and development of a semipredictive model. *Journal of Rheology, 63*(1), 179–190. https://doi.org/10.1122/1.5062837

Scott, G. D., & Kilgour, D. M. (1969). The density of random close packing of spheres. *Journal of Physics D: Applied Physics, 2*(6), 863–866. https://doi.org/10.1088/0022-3727/2/6/311

Seth, J. R., Mohan, L., Locatelli-Champagne, C., Cloitre, M., & Bonnecaze, R. T. (2011). A micromechanical model to predict the flow of soft particle glasses. *Nature Materials, 10*(11), 838–843. https://doi.org/10.1038/nmat3119

Sosa-Herrera, M. G. G., Lozano-Esquivel, I. E. E., Ponce de León-Ramírez, Y. R. R., & Martínez-Padilla, L. P. P. (2012). Effect of added calcium chloride on the physicochemical and rheological properties of aqueous mixtures of sodium caseinate/sodium alginate and respective oil-in-water emulsions. *Food Hydrocolloids, 29*(1), 175–184. https://doi.org/10.1016/j.foodhyd.2012.02.017

Su, J., Wang, X., Li, W., Chen, L., Zeng, X., Huang, Q., & Hu, B. (2018). Enhancing the Viability of lactobacillus plantarum as probiotics through encapsulation with high internal phase emulsions stabilized with whey protein isolate microgels. *Journal of Agricultural and Food Chemistry, 66*(46), 12335–12343. https://doi.org/10.1021/acs.jafc.8b03807

Tadros, T. F. (1994). Fundamental principles of emulsion rheology and their applications. *Colloids and Surfaces A: Physicochemical and Engineering Aspects, 91*, 39–55. https://doi.org/10.1016/0927-7757(93)02709-N

Tadros, T. (2004). Application of rheology for assessment and prediction of the long-term physical stability of emulsions. *Advances in Colloid and Interface Science, 108*(109), 227–258. https://doi.org/10.1016/j.cis.2003.10.025

Tang, Y. R., & Ghosh, S. (2021). Stability and rheology of canola protein isolate-stabilized concentrated oil-in-water emulsions. *Food Hydrocolloids, 113*(October 2020), Article 106399. https://doi.org/10.1016/j.foodhyd.2020.106399

Tan, Y., Zhang, Z., Muriel Mundo, J., & McClements, D. J. (2020). Factors impacting lipid digestion and nutraceutical bioaccessibility assessed by standardized gastrointestinal model (INFOGEST): Emulsifier type. *Food Research International, 137*, Article 109739. https://doi.org/10.1016/j.foodres.2020.109739

Tomas, A., Paquet, D., Courthaudon, J. L., & Lorient, D. (1994). Effect of fat and protein contents on droplet size and surface protein coverage in dairy emulsions. *Journal of Dairy Science, 77*(2), 413–417. https://doi.org/10.3168/jds.S0022-0302(94)76967-8

Wang, A. J., Paterson, T., Owen, R., Sherborne, C., Dugan, J., Li, J. M., & Claeyssens, F. (2016). Photocurable high internal phase emulsions (HIPEs) containing hydroxyapatite for additive manufacture of tissue engineering scaffolds with multi-scale porosity. *Materials Science and Engineering: C, 67*, 51–58. https://doi.org/10.1016/j.msec.2016.04.087

Wijaya, W., Patel, A. R., Setiowati, A. D., & Van der Meeren, P. (2017). Functional colloids from proteins and polysaccharides for food applications. *Trends in Food Science and Technology, 68*, 56–69. https://doi.org/10.1016/j.tifs.2017.08.003

Wilking, J. N., & Mason, T. G. (2007). Irreversible shear-induced vitrification of droplets into elastic nanoemulsions by extreme rupturing. *Physical Review E, 75*(4), Article 041407. https://doi.org/10.1103/PhysRevE.75.041407

Williams, R. P. W., D'Ath, L., & Augustin, M. A. (2005). Production of calcium-fortified milk powders using soluble calcium salts. *Le Lait, 85*(4–5), 369–381. https://doi.org/10.1051/lait:2005011

Xu, Y. T., Liu, T. X., & Tang, C. H. (2019). Novel pickering high internal phase emulsion gels stabilized solely by soy β-conglycinin. *Food Hydrocolloids, 88*, 21–30. https://doi.org/10.1016/j.foodhyd.2018.09.031

Xu, Y. T., Tang, C. H., Liu, T. X., & Liu, R. (2018). Ovalbumin as an outstanding Pickering nanostabilizer for high internal phase emulsions. *Journal of Agricultural and Food Chemistry, 66*(33), 8795–8804. https://doi.org/10.1021/acs.jafc.8b02183

Yang, F., Niu, Q., Lan, Q., & Sun, D. (2007). Effect of dispersion pH on the formation and stability of Pickering emulsions stabilized by layered double hydroxides particles. *Journal of Colloid and Interface Science, 306*(2), 285–295. https://doi.org/10.1016/j.jcis.2006.10.062

Yan, C., McClements, D. J., Zhu, Y., Zou, L., Zhou, W., & Liu, W. (2019). Fabrication of OSA starch/chitosan polysaccharide-based high internal phase emulsion via altering interfacial behaviors. *Journal of Agricultural and Food Chemistry, 67*(39), 10937–10946. https://doi.org/10.1021/acs.jafc.9b04009

Ye, A., Zhu, X., & Singh, H. (2013). Oil-in-water emulsion system stabilized by protein-coated nanoemulsion droplets. *Langmuir, 29*(47), 14403–14410. https://doi.org/10.1021/la403493y

Zeng, T., Wu, Z. ling, Zhu, J. Y., Yin, S. W., Tang, C. H., Wu, L. Y., & Yang, X. Q. (2017). Development of antioxidant Pickering high internal phase emulsions (HIPEs) stabilized by protein/polysaccharide hybrid particles as potential alternative for PHOs. *Food Chemistry, 231*, 122–130. https://doi.org/10.1016/j.foodchem.2017.03.116

Zhang, R., Cheng, L., Luo, L., Hemar, Y., & Yang, Z. (2021). Formation and characterisation of high-internal-phase emulsions stabilised by high-pressure homogenised quinoa protein isolate. *Colloids and Surfaces A: Physicochemical and Engineering Aspects, 631*, Article 127688. https://doi.org/10.1016/j.colsurfa.2021.127688

Zhang, S., Holmes, M., Ettelaie, R., & Sarkar, A. (2020a). Pea protein microgel particles as pickering stabilisers of oil-in-water emulsions: Responsiveness to pH and ionic strength. *Food Hydrocolloids, 102*, Article 105583. https://doi.org/10.1016/j.foodhyd.2019.105583

Zhang, X., Luo, X., Wang, Y., Li, Y., Li, B., & Liu, S. (2020b). Concentrated O/W pickering emulsions stabilized by soy protein/cellulose nanofibrils: Influence of pH on the emulsification performance. *Food Hydrocolloids, 108*, Article 106025. https://doi.org/10.1016/j.foodhyd.2020.106025

Zheng, X., Zhang, Y., Wang, H., & Du, Q. (2014). Interconnected macroporous polymers synthesized from silica particle stabilized high internal phase emulsions. *Macromolecules, 47*(19), 6847–6855. https://doi.org/10.1021/ma501253u

Zhou, F.-Z., Huang, X.-N., Wu, Z., Yin, S.-W., Zhu, J., Tang, C.-H., & Yang, X.-Q. (2018). Fabrication of zein/pectin hybrid particle-stabilized Pickering high internal phase emulsions with robust and ordered interface architecture. *Journal of Agricultural and Food Chemistry, 66*(42), 11113–11123. https://doi.org/10.1021/acs.jafc.8b03714

Zhu, Y., Gao, H., Liu, W., Zou, L., & McClements, D. J. (2019). A review of the rheological properties of dilute and concentrated food emulsions. *Journal of Texture Studies, 51*(1). https://doi.org/10.1111/jtxs.12444. jtxs.12444.

Zittle, C. A., DellaMonica, E. S., Rudd, R. K., & Custer, J. H. (1958). Binding of calcium to casein: Influence of pH and calcium and phosphate concentrations. *Archives of Biochemistry and Biophysics, 76*(2), 342–353. https://doi.org/10.1016/0003-9861(58)90159-0